

Article

Hybridizing neural network with multi-verse, black hole, and shuffled complex evolution optimizer algorithms predicting the dissolved oxygen

Hossein Moayed ^{1,2}, Amir Mosavi ^{3,4},

1 Institute of Research and Development, Duy Tan University, Da Nang, 550000, Viet Nam;
hosseinmoayed@duytan.edu.vn

2 Faculty of Civil Engineering, Duy Tan University, Da Nang 550000, Vietnam.

3 School of Economics and Business, Norwegian University of Life Sciences, 1430 Ås, Norway,
a.mosavi@ieee.org

4 John von Neumann Faculty of Informatics, Obuda University, 1034 Budapest, Hungary

Abstract: The great importance of estimating dissolved oxygen (DO) dictates utilizing proper evaluative models. In this work, a multi-layer perceptron (MLP) network is trained by three capable metaheuristic algorithms, namely multi-verse optimizer (MVO), black hole algorithm (BHA), and shuffled complex evolution (SCE) for predicting the DO using the data of the Klamath River Station, Oregon, US. The records (DO, water temperature, pH, and specific conductance) belonging to the water years 2015 - 2018 (USGS) are used for pattern analysis. The results of this process showed that all three hybrid models could properly infer the DO behavior. However, the BHA and SCE accomplished this task by simpler configurations. Next, the generalization ability of the developed patterns is tested using the data of the 2019 water year. Referring to the calculated mean absolute errors of 1.0161, 1.1997, and 1.0122, as well as Pearson correlation coefficients of 0.8741, 0.8453, and 0.8775, the MLPs trained by the MVO and SCE perform better than the BHA. Therefore, these two hybrids (i.e., the MLP-MVO and MLP-SCE) can be satisfactorily used for future applications.

Keywords: Water quality; dissolved oxygen; Neural network; Metaheuristic schemes.

1 Introduction

As is known, acquiring an appropriate forecast from water quality parameters like dissolved oxygen (DO) is an important task due to their effects on aquatic health maintenance and reservoir management [1]. The constraints like the influence of various environmental factors on the DO concentration [2] have driven many scholars to replace the conventional models with sophisticated artificial intelligent techniques [3-6]. As discussed by many scholars, intelligence techniques have a high capability to undertake non-linear and complicated calculations [7-14]. A large number artificial intelligence-based practices are studied, for example, in the subjects of environmental concerns [15-21], sustainability [22], quantifying climatic contributions [23], pan evaporation and soil precipitation prediction [22, 24, 25], air quality [26], optimizing energy systems [27-34], water and groundwater supply chains [17, 35-43], natural gas consumption [44], face or particular pattern

recognition [23, 45-49], image classification and processing [50, 51], target tracking and computer vision [41, 52-57], structural health monitoring [58, 59], building and structural design analysis [58, 60-62], structural material (e.g., steel and concrete) behaviors [8, 21, 61, 63-67], soil-pile analysis and landslide assessment [12, 67-70], seismic analysis [70-72], measurement techniques [41, 59, 60, 73], or very complex problems such as signal processing [50, 52, 74, 75] as well as feature selection and extraction problems [23, 50, 74, 76-78]. Similar to deep learning-based applications [53, 73, 79-83], many decision-making applications work related to engineering complicated problems as well [60, 84-89].

A neural network is known as a series of complex algorithms that recognize underlying connections in a set of data input and outputs through a process that mimics the way the human brain operates [45, 46, 90-93]. In another sense, the technique of artificial neural network (ANN) is a sophisticated nonlinear processor that has attracted massive attention for sensitive engineering modeling [94]. Different notions represent this model. Most importantly, a multi-layer perceptron (MLP) [81, 95] is composed of a minimum of three layers, each of which contains some neurons for handling the computations - noting that a more complicated ANN-based solution is known as deep learning [96, 97] where it refers as part of a wider family of conventional training machine technique based on ANN with representation learning [79, 80, 82, 83, 98]. For instance, Chen, et al. [99], Hu, et al. [100], Wang, et al. [47], and Xia, et al. [101] employed the use of extreme machine learning techniques in the field of medical sciences. As some new advanced prediction techniques, hybrid searching algorithms are widely developed to have more accurate prediction outputs; namely, harris hawks optimization [67], enhanced grey wolf optimization [102], multiobjective large-scale optimization [40, 90, 103, 104], fruit fly optimization [105], multi-swarm whale optimizer [13], ant colony optimization [106], as well as conventional and extreme machine learning-based solutions [107-111].

Through applying a support vector regression (SVR), Li, et al. [112] showed the efficiency of the maximal information coefficient technique used for feature selection in the estimation of the DO concentration. The results of the optimized dataset were much more reliable (28.65% in terms of root mean square error, RMSE) than the original input configuration. Csábrági, et al. [113] showed the appropriate efficiency of three conventional notions of artificial neural networks (ANNs) by the names multilayer perceptron (MLP), radial basis function (RBF), and general regression neural network (GRNN) for this purpose. Similar efforts can be found in [114, 115]. Heddad [116] introduced a new ANN-based model, namely evolving fuzzy neural network as a capable approach for the DO simulation in the river ecosystem. The suitability of fuzzy-based models has been investigated in many studies [117]. Adaptive neuro-fuzzy inference system (ANFIS) is another potent data mining technique that has been discussed in many studies [118-120]. More attempts regarding the employment of machine learning tools can be found in [121-124].

Ouma, et al. [125] compared the performance of a feed-forward ANN with multiple linear regression (MLR) in simulating the DO in Nyando River, Kenya. It was shown that the correlation of the ANN is considerably greater than the MLR (i.e., 0.8546 vs. 0.6199). Zhang and Wang [58] combined a recurrent neural network (RNN) with kernel principal component analysis (kPCA) to predict the hourly DO concentration. Their suggested model was found to be more accurate than traditional data mining techniques, including feed-forward ANN, SVR, and GRNN by around 8, 17, and 12%. The most considerable accuracy

(the coefficient of determination (R^2) = 0.908) was obtained for the DO in the upcoming one hour. Lu and Ma [126] combined a so-called denoising method “complete ensemble empirical mode decomposition with adaptive noise” with two popular machine learning models, namely random forest (RF) and extreme gradient boosting (XGBoost) to analyze various water quality parameters. It was shown that the RF-based ensemble is a more accurate approach for the simulation of DO, temperature, and specific conductance. They also proved the viability of the proposed approaches by comparing them with some benchmark tools. Likewise, Ahmed [127] showed the superiority of the RF over the MLR for DO modeling. He also revealed that water temperature as well as pH play the most significant role in this process. Ay and Kişi [128] conducted a comparison among MLP, RBF, ANFIS (sub-clustering), and ANFIS (grid partitioning). Respective R^2 values of 0.98, 0.96, 0.95, and 0.86 for one station (Number: 02156500) revealed that the outcomes of the MLP are better-correlated with the observed DOs.

Synthesizing conventional approaches with auxiliary techniques has led to novel hybrid tools for various hydrological parameters [129-131]. Ravansalar, et al. [132] showed that linking the ANN with a discrete wavelet transform results in improving the accuracy (i.e., Nash–Sutcliffe coefficient) from 0.740 to 0.998. A similar improvement was achieved for the SVR applied to estimate biochemical oxygen demand in Karun River, Western Iran. Antanasijević, et al. [133] presented a combination of Ward neural networks and local similarity index for predicting the DO in the Danube River. They stated the better performance of the proposed model compared to multisite DO evaluative approaches presented in the literature. Metaheuristic search methods, like teaching-learning based optimization [134], have provided suitable approaches for intricate problems. Ahmed and Shah [118] suggested three optimized versions of ANFIS using differential evolution, genetic algorithm (GA), and ant colony optimization for predicting water quality parameters, including electrical conductivity, sodium absorption ratio, and total hardness. In similar research, Mahmoudi, et al. [135] coupled the SVR with shuffled frog leaping algorithm (SFLA) for the same objective. Zhu, et al. [136] compared the efficiency of the fruit fly optimization algorithm (FOA) with the GA and particle swarm optimization (PSO) for optimizing a least-squares SVR for forecasting the trend of DO. Referring to the obtained mean absolute percentage errors of 0.35, 1.3, 2.03, and 1.33%, the proposed model (i.e., FOA-LSSVR) surpassed the benchmark techniques. In this work, three stochastic search techniques of multi-verse optimizer (MVO), black hole algorithm (BHA), and shuffled complex evolution (SCE) are used to optimize an MLP neural network for predicting the DO using recent data collected from the Klamath River Station. To the best of the authors’ knowledge, up to now, a few metaheuristic algorithms have been used for training the ANN in the field of DO modeling (e.g., firefly algorithm [137] and PSO [138]). Therefore, the models suggested in this study are deemed as innovative hybrids for this purpose.

2 Data

As a matter of fact, intelligent models should first learn the pattern of the intended parameter to predict it. This learning process is carried out by analyzing the dependence of the target parameter on some independent factors. In this work, the DO is the target parameter for water temperature (WT), pH, and specific conductance (SC). This study uses the data belonging to a US Geological Survey (USGS) station, namely the Klamath River

(station number: 11509370). As Figure 1 illustrates, this station is located in Klamath County, Oregon State.



Figure 1: Location of the studied USGS station.

Pattern recognition is fulfilled by means of the data between October 01, 2014, and September 30, 2018. After training the models, they predict the DO for the subsequent year (i.e., from October 01, 2018, to September 30, 2019). Since the models do not know this data, the accuracy of this process will reflect their capability for predicting the DO in unseen conditions. Hereafter, these two groups are categorized as training data and testing data, respectively. Figure 2 depicts the DO versus WT, PH, and SC for the (a, c, and e) training and (b, d, and f) testing data. Based on the available data for the mentioned periods, the training and testing groups contain 1430 and 352 records, respectively. Moreover, the statistical description of these datasets is presented in Table 1.

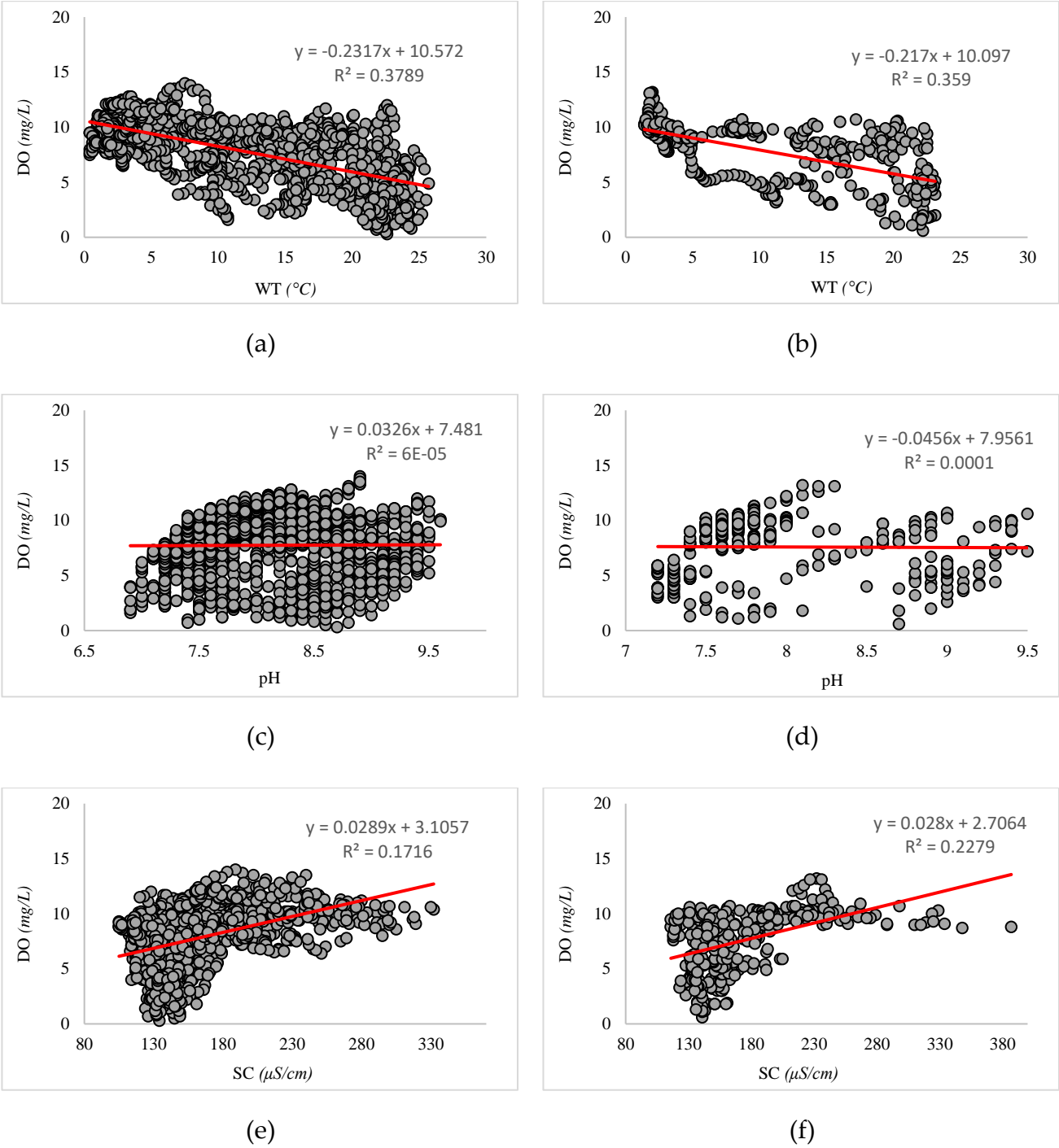


Figure 2: Scatterplots showing the DO vs. independent factors.

Table 1: Statistical indicators of the DO and independent factors.

Indicator	Train data				Test data			
	WT (°C)	pH	SC ($\mu S/cm$)	DO (mg/L)	WT (°C)	pH	SC ($\mu S/cm$)	DO (mg/L)
Average	12.20	8.05	160.46	7.74	11.54	7.97	174.20	7.59
Standard Deviation	7.38	0.64	39.81	2.78	7.43	0.65	45.80	2.69
Sample Variance	54.43	0.41	1584.75	7.72	55.23	0.42	2097.97	7.24
Skewness	0.07	0.48	1.54	-0.54	0.11	0.96	1.49	-0.57
Minimum	0.40	6.90	105.00	0.30	1.40	7.20	116.00	0.60
Maximum	25.70	9.60	332.00	14.00	23.10	9.60	387.00	13.20

3 Methodology

The steps of this research are shown in Figure 3. After providing the appropriate dataset, the MLP is submitted to the MVO, BHA, and SCE algorithms for adjusting its parameters through metaheuristic schemes. During an iterative process, the MLP is optimized to present the best possible prediction of the DO. The quality of the results is lastly evaluated using Pearson correlation coefficient (R_p) along with mean absolute error (MAE) and RMSE. They analyze the agreement and the difference between the observed and predicted values of a target parameter. In the present work, given $DO_{i_{predicted}}$ and $DO_{i_{observed}}$ as the predicted and observed DOs, the R_p , MAE, and RMSE are expressed by the following equations:

$$R_p = \frac{\sum_{i=1}^K (DO_{i_{predicted}} - \overline{DO}_{predicted})(DO_{i_{observed}} - \overline{DO}_{observed})}{\sqrt{\sum_{i=1}^K (DO_{i_{predicted}} - \overline{DO}_{predicted})^2} \sqrt{\sum_{i=1}^K (DO_{i_{observed}} - \overline{DO}_{observed})^2}} \quad (1)$$

$$MAE = \frac{1}{Q} \sum_{i=1}^K |DO_{i_{observed}} - DO_{i_{predicted}}| \quad (2)$$

$$RMSE = \sqrt{\frac{1}{K} \sum_{i=1}^K [(DO_{i_{observed}} - DO_{i_{predicted}})]^2} \quad (3)$$

where K signifies the number of the compared pairs.

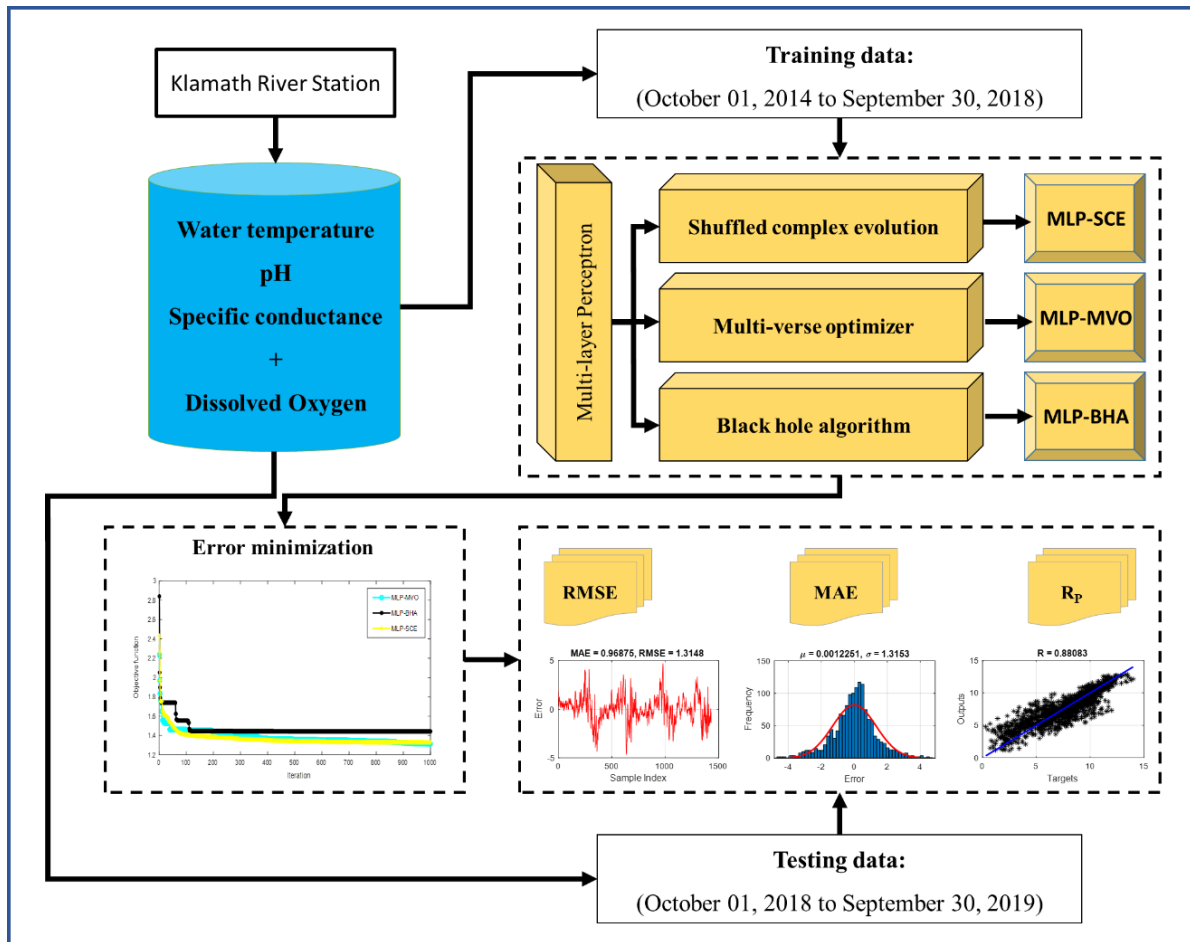


Figure 3: The steps of this research taken for predicting the DO.

3.1 The MVO

As is implied by its name, the MVO is obtained from multi-verse theory in physics [139]. According to this theory, there is more than one big bang event, each of which has initiated a separate universe. The algorithm was introduced by Mirjalili, et al. [140]. The main components of the MVO are worm holes, black holes, and white holes. The concepts of black and white holes run the exploration phase, while the wormhole concept is dedicated to the exploitation procedure.

In the MVO, a so-called parameter “rate of inflation (ROI)” is defined for each universe. The objects are transferred from the universes with larger ROIs to those with lower values for improving the whole cosmos' average ROI. During an iteration, the organization of the universes is carried out with respect to their ROIs, and after a roulette wheel selection (RWS), one of them is deemed as the white hole. In this relation, a set of universes can be defined as:

$$U = \begin{bmatrix} x_1^1 & x_1^2 & \dots & x_1^g \\ x_2^1 & x_2^2 & \dots & x_2^g \\ \vdots & \vdots & \vdots & \vdots \\ x_k^1 & x_k^2 & \dots & x_k^g \end{bmatrix} \quad (4)$$

where g symbolizes the number of objects and k stands for the number of universes. The j^{th} objective in the i^{th} solution is generated according to the below equation:

$$x_i^j = lb_j + rand() \% ((ub_j - lb_j) + 1) \quad \forall i \in (1, 2, \dots, k) \wedge \forall j \in (1, 2, \dots, g) \quad (5)$$

where ub_j and lb_j denote upper and lower bounds, and the function $rand()$ produces a discrete randomly distributed number.

In each repetition, there are two options for the x_i^j : (i) it is selected from earlier solutions using RWS (e.g., $x_i^j \in (x_i^1, x_i^2, \dots, x_i^{j-1})$) and (ii) it does not change. It can be written:

$$x_i^j = \begin{cases} x_m^j & rand_1 < Norm(U_i) \\ x_i^j & rand_1 \geq Norm(U_i) \end{cases} \quad (6)$$

In the above equation, U_i stands for the i^{th} universe, $Norm(U_i)$ gives the corresponding normalized ROI, and $rand_1$ is a random value in $[0, 1]$.

Equation 7 expresses the measures considered to deliver the variations of the whole universe. In this sense, the wormholes are supposed to enhance the ROI.

$$x_i^j = \begin{cases} \begin{cases} x_j + TDR \times ((ub_j - lb_j) \times r_4 + lb_j) & \text{if } r_3 < 0.5 \\ x_j - TDR \times ((ub_j - lb_j) \times r_4 + lb_j) & \text{if } r_3 \geq 0.5 \end{cases} & \text{if } r_2 < WEP \\ x_i^j & \text{if } r_2 \geq WEP \end{cases} \quad (7)$$

where x_j signifies the j^{th} best-fitted universe obtained so far and r_2 , r_3 , and r_4 are random values in $[0, 1]$. Moreover, two parameters of WEP and TDR stand for the wormhole existence probability and traveling distance rate, respectively. Given $Iter$ as the running iteration, and $Iter_{max}$ as the maximum number of $Iters$, these parameters can be calculated as follows:

$$WEP = a + Iter \times \left(\frac{b-a}{Iter_{max}} \right) \quad (8)$$

$$TDR = 1 - \frac{Iter^{1/q}}{Iter_{max}^{1/q}} \quad (9)$$

where q is the accuracy of exploitation, a and b are constant pre-defined values [141, 142].

3.2 The BHA

Inspired by the black holes incidents in space, Hatamlou [143] proposed the BHA in 2013. Emerged after the collapse of massive stars, a black hole is distinguished by a huge gravitational power. The stars move toward this mass, and it explains the pivotal strategy of the BHA for achieving an optimum response. A randomly generated constellation of stars represents the initial population. Based on the fitness of these stars, the most powerful one is deemed as the black hole to absorb the surrounding ones. In this procedure, the positions change according to the below relationship:

$$x_i^{Iter+1} = x_i^{Iter} + rand \times (x_{BH} - x_i^{Iter}) \quad i = 1, 2, \dots, Z \quad (10)$$

where $rand$ is a random number in $[0, 1]$, x_{BH} is the black hole's position, Z is the total number of stars, and $Iter$ symbolizes the iteration number.

Once the fitness of a star surpasses that of the black hole, they exchange their positions. In this regard, Equation 11 calculates the radius of the event horizon for the black hole.

$$R_S = F_{BH} / \sum_{i=1}^Z F_i \quad (11)$$

where F_i is the fitness of the i^{th} star and F_{BH} gives this value for the black hole [144].

3.3 The SCE

Originally proposed by Duan, et al. [145], the SCE has been efficiently used for dealing with optimization problems with high dimensions. The SCE can be defined as a hybrid of complex shuffling and competitive evolution concepts along with the strengths of the controlled random search strategy. This algorithm (i.e., the SCE) benefits from a deterministic strategy to guide the search. Also, utilizing random elements has resulted in a flexible and robust algorithm.

In the SCE is implemented in seven steps. Assuming N_C as the number of complexes and N_P as the number of points existing in one complex, the sample size of the algorithm is generated as $S = N_C \times N_P$. In this sense, $N_C \geq 1$ and $N_P \geq 1 + \text{the number of design variables}$. Next, the samples x_1, x_2, \dots, x_s is created in the viable space (i.e., within the bounds). The fitness values are also calculated using sampling distribution. In the third step, these samples are arranged with reference to their fitness. An array-like $D = \{x_i, f_i, \text{ where } i = 1, 2, \dots, s\}$ can be considered for storing them. This array is then divided into N_C complexes (C^1, C^2, \dots, C^{N_C}) each of which containing N_P samples (Equation 12)

$$C^q = \{x_j^q, f_j^q \mid x_j^q = x_{q+N_C(j-1)}, f_j^q = f_{q+N_C(j-1)}, j = 1, 2, \dots, N_P\}. \quad (12)$$

In the fifth step, each complex is evolved by the competitive complex evolution algorithm. Later, in a process named shuffling of the complexes, all complexes are replaced in the array D . This array is then sorted based on the fitness values. Lastly, the algorithm checks for stopping criteria to terminate the process [146].

4 Results and discussion

4.1 Optimization and weight adjustment

As explained, the proposed hybrid models are designed in the way that MVO, BHA, and SCE algorithms are responsible for adjusting the weights and biases of the MLP. Each algorithm first suggests a stochastic response to re-build the MLP. In the next iterations, the algorithms improve this response to build a more accurate MLP. In this relation, the overall formulation of the MLP that is applied to the training data can be expressed as follows:

$$R_N = f(I_N \times W + b) \quad (13)$$

where $f(x)$ is the activation function used by the neurons in a layer, also, R_N and I_N denote the response and the input of the neuron N , respectively.

The created hybrids are implemented with different population sizes (N_{PopS}) for achieving the best results. Figure 4 shows the values of the objective function obtained for the N_{PopS} of 10, 25, 50, 75, 100, 200, 300, 400, and 500. In the case of this study, the objective function is reported by the RMSE criterion. Figure 4 says that unlike the SCE, which gives more quality training with small N_{PopS} , the MVO performs better with the three largest N_{PopS} . The BHA,

however, did not show any specific behavior. Overall, the MVO, BHA, and SCE with the N_{Pop} s of 300, 50, and 10, respectively, could adjust the MLP parameters with the lowest error.

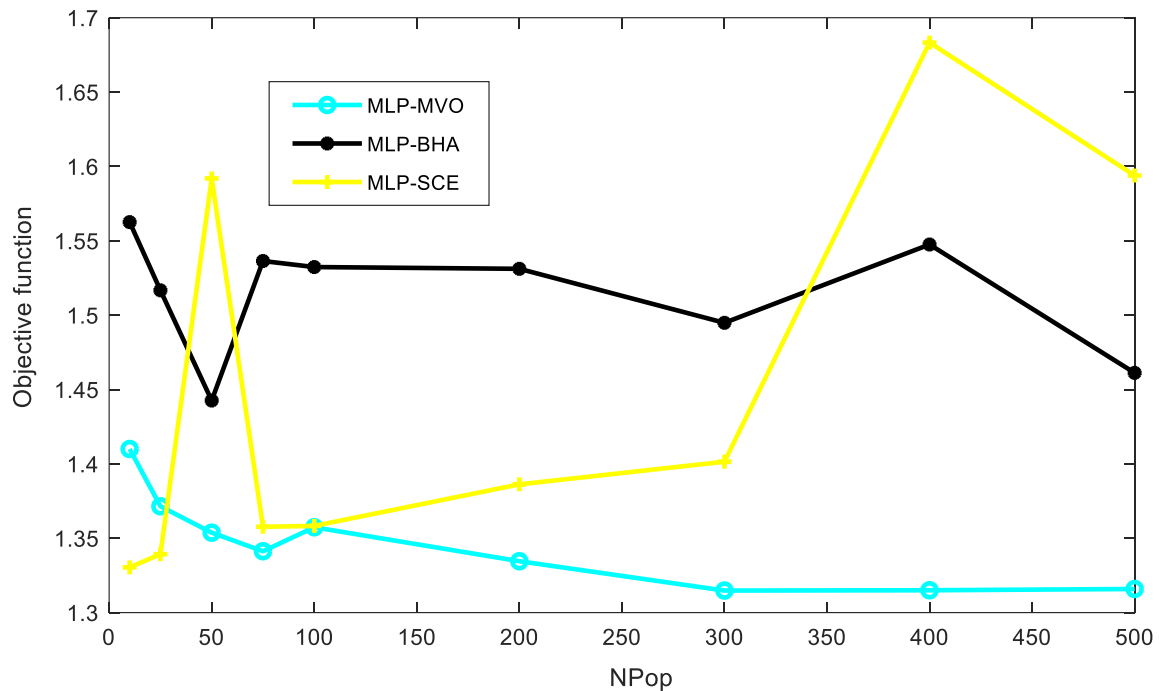


Figure 4: The quality of training for different configurations of the MVO, BHA, and SCE.

As stated, metaheuristic algorithms minimize the error in an iterative process. Figure 5 shows the convergence curve plotted for the selected configurations of the MLP-MVO, BHA-MVO, and SCE-MVO. To this end, the training RMSE is calculated for a total of 1000 iterations. According to Figure 5, the optimum values of the objective function are 1.314816444, 1.442582978, and 1.33041779 for the MLP-MVO, BHA-MVO, and SCE-MVO, respectively. These configurations are applied in the next section to predict the DO. Their results are then evaluated for accuracy assessment.

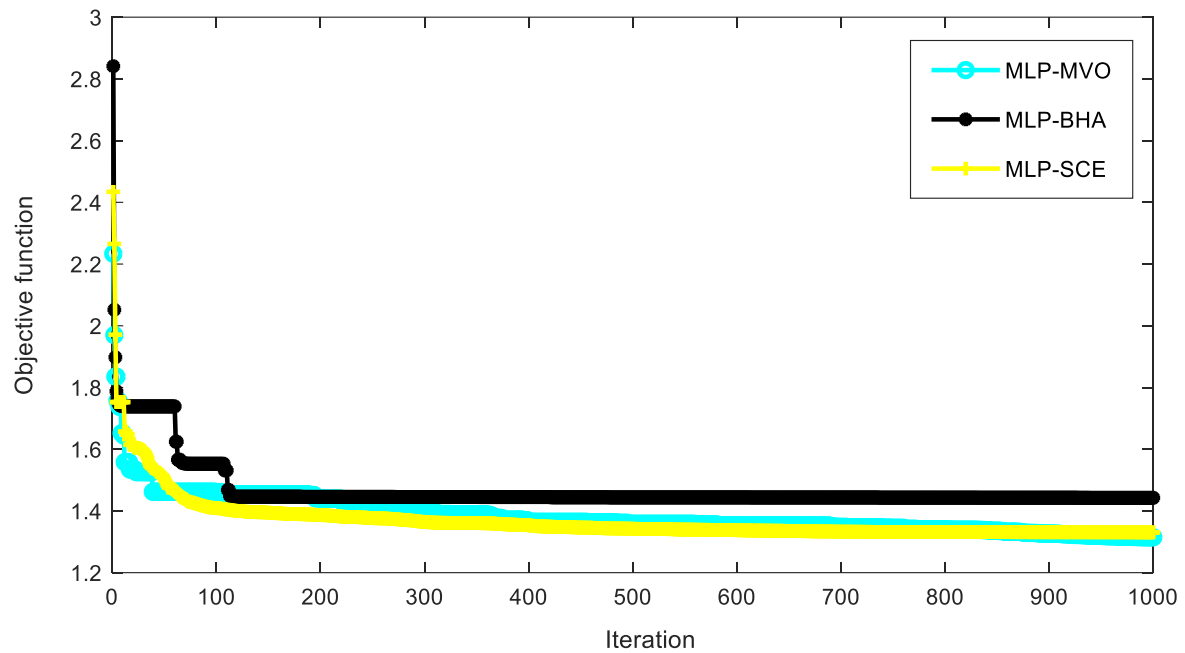


Figure 5: Error reduction carried out by the selected configurations of the MVO, BHA, and SCE.

4.2 Assessment of the results

Figure 6 shows a comparison between the observed DOs and those predicted by the MLP-MVO, MLP-BHA, and MLP-SCE for the whole five years. At a glance, all three models could properly capture the DO behavior. It indicates that the algorithms have designated appropriate weights for each input parameter (WT, PH, and SC). The results of the training and testing datasets are presented in detail in the following.

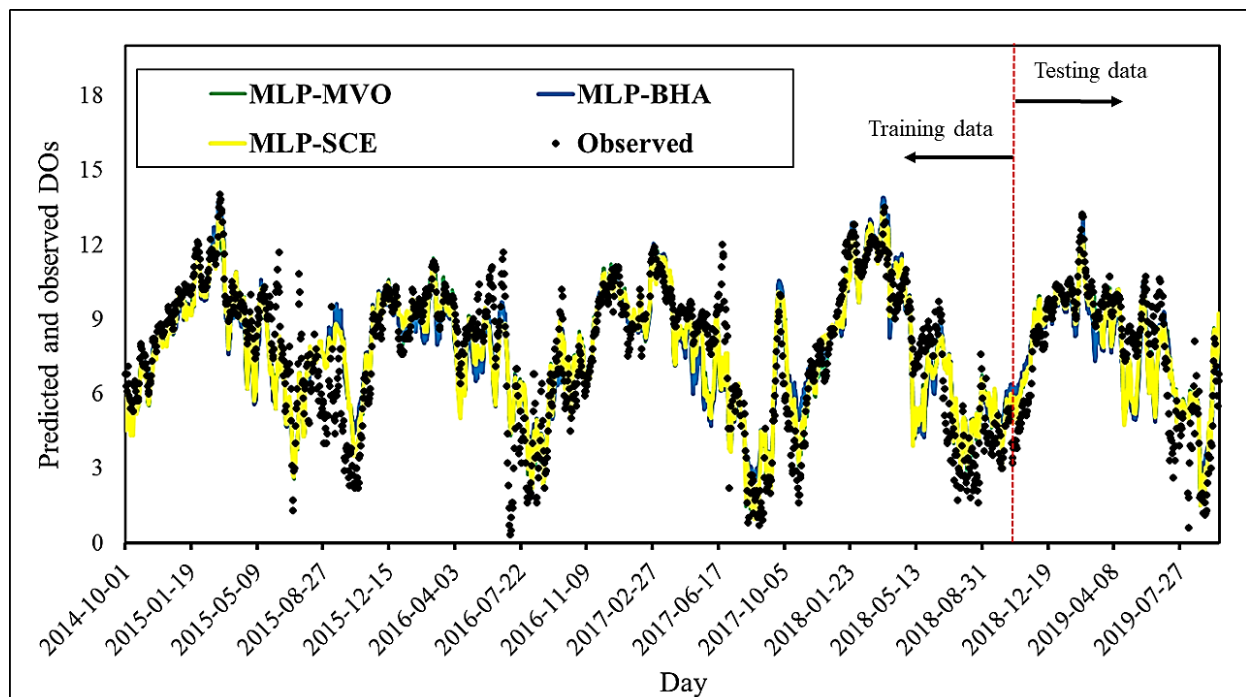


Figure 6: The predicted and observed DOs from October 01, 2014 to September 30, 2019.

Focusing on the training results, an acceptable level of accuracy is reflected by the RMSEs of 1.3148, 1.4426, and 1.3304 for the MLP-MVO, MLP-BHA, and MLP-SCE. In this sense, the values of the MAE (0.9687, 1.0931, and 0.9929) confirmed this statement and showed all three models had understood the DO pattern with good accuracy. By comparison, it can be deduced that both error values of the MLP-MVO are lower than the two other models. Based on the same reason, the MLP-SCE outperformed the MLP-BHA.

Figure 7 depicts the errors obtained for the training data. This value is calculated as the difference between the predicted and observed DOs. The errors of the MLP-MVO, MLP-BHA, and MLP-SCE range in $[-4.6396, 4.7003]$, $[-4.4964, 4.9537]$, and $[-4.5585, 4.5653]$.

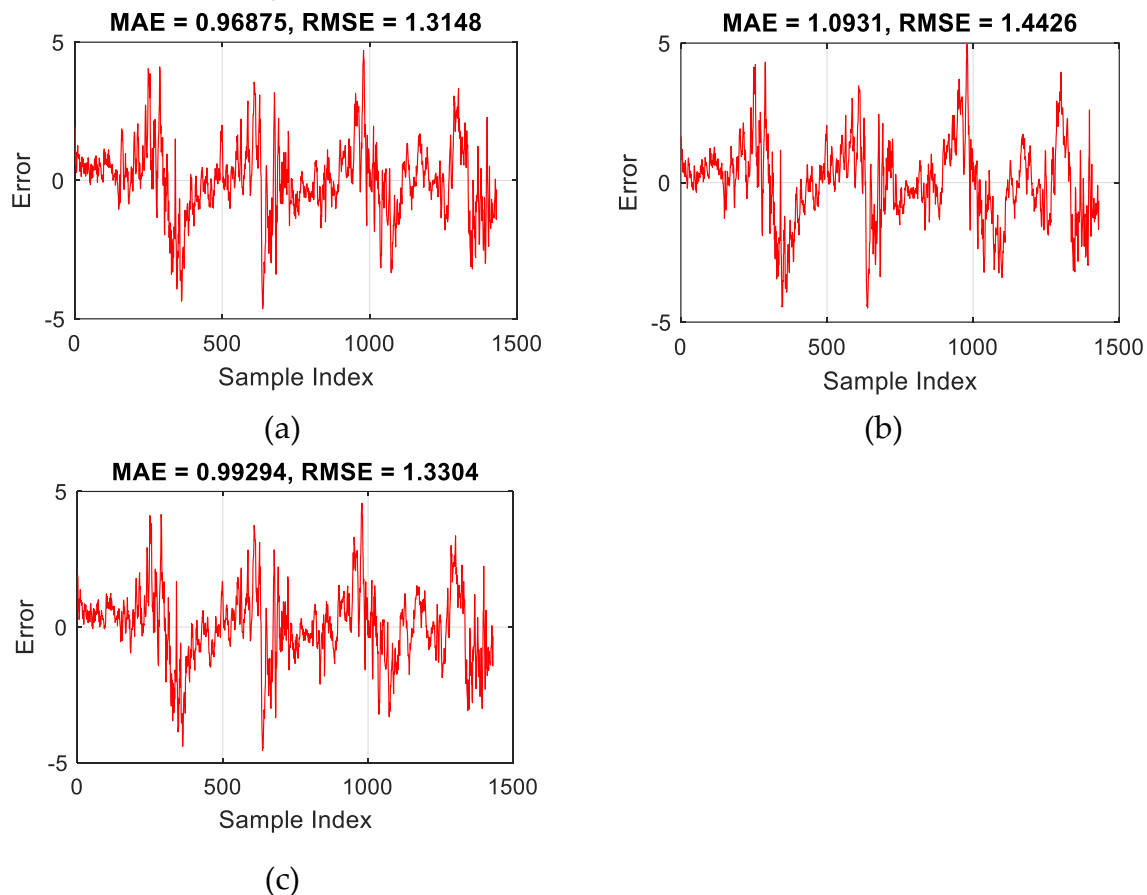


Figure 7: Training errors for the (a) MLP-MVO, (b) MLP-BHA, and (c) MLP-SCE.

As stated previously, the quality of the testing results shows how successful a trained model can be in confronting new conditions. The data of the fifth year were considered as these conditions in this study. Figure 8 depicts the histogram of the testing errors. In these charts, μ stands for the mean error, and σ represents the standard error. In this phase, the RMSEs of 1.3187, 1.4647, and 1.3085, along with the MEAs of 1.0161, 1.1997, and 1.0122, implied the power of the used models for dealing with stranger data. It means that the weights (and biases) determined in the previous section have successfully mapped the relationship between the DO and WT, PH, and SC for the second phase. From the comparison point of view, unlike the training phase, the SCE-based hybrid outperformed the MLP-MVO. The MLP-BHA, however, presented the poorest prediction of the DO again.

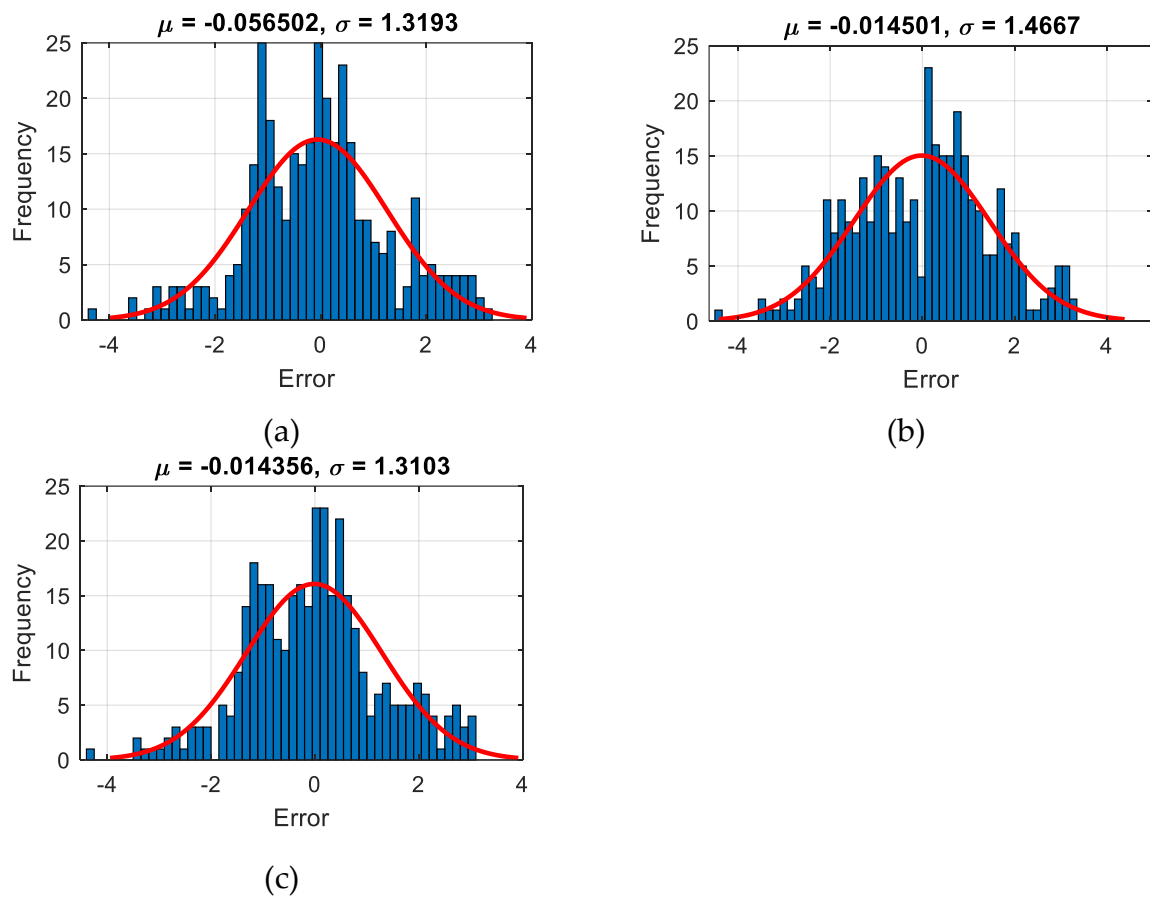


Figure 8: The histogram of the testing errors for the (a) MLP-MVO, (b) MLP-BHA, and (c) MLP-SCE.

The third accuracy indicator (i.e., the R_F) shows the agreement between the predicted and observed DOs. This index can range in $[-1, +1]$ where -1 (+1) indicates a totally negative (positive) correlation, and 0 means no correlation. Figure 9 shows a scatterplot for each model containing both training and testing results. As is seen, all outputs are positively aggregated around the best-fit line (i.e., the black line). For the training results, the R_F s of 0.8808, 0.8545, and 0.8778 indicate the higher consistency of the MLP-MVO results, while the values of 0.8741, 0.8453, and 0.8775 demonstrate the superiority of the MLP-SCE in the testing phase.

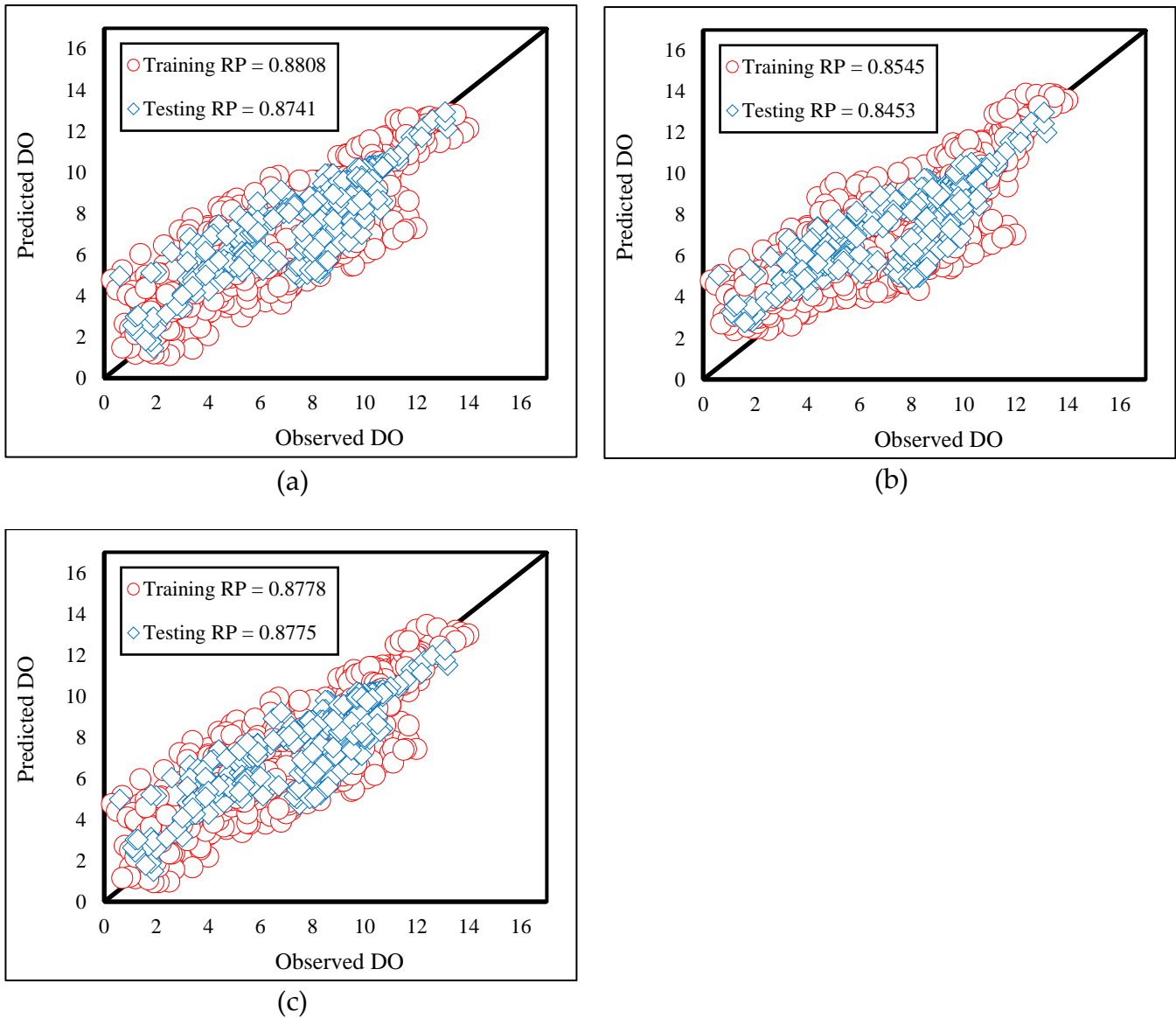


Figure 9: The error line and scatterplot plotted for the testing data of (a) MLP-MVO, (b) MLP-BHA, and (c) MLP-SCE.

5 Conclusions

This research pointed out the suitability of metaheuristic strategies for analyzing the relationship between the DO and three influential factors (WT, PH, and SC) through the principals of a multi-layer perceptron network. The used algorithms were multi-verse optimizer, black hole algorithm, and shuffled complex evolution, which has shown high applicability for optimization objectives. A finding of this study was that while the MVO needs $N_{pop} = 300$ to give a proper training of the MLP, two other algorithms can do this with smaller populations (N_{pop} s of 50 and 10). According to the findings of the training phase, the MVO can achieve a more profound understanding of the mentioned relationship. The RMSE of this mode was 1.3148, which was found to be smaller than MLP-BHA (1.4426) and MLP-SCE (1.3304). But different results were observed in the testing phase. The SCE-based model came up with the largest accuracy (the RPs were 0.8741, 0.8453, and 0.8775). All in all, the authors believe that the tested models can serve as promising ways for predicting the DO.

However, assessing other metaheuristic techniques and other hybridization strategies is recommended for future studies.

Author Contributions: H.M. methodology; software validation, writing—original draft preparation, A.M. writing—review and editing, visualization, supervision, project administration. All authors have read and agreed to the published version of the manuscript.

Funding: This research was not funded

Conflicts of Interest: The authors declare no conflict of interest.

6 References

1. Kisi, O.; Alizamir, M.; Gorgij, A. D., Dissolved oxygen prediction using a new ensemble method. *Environmental Science and Pollution Research* **2020**, 1-15.
2. Liu, S.; Yan, M.; Tai, H.; Xu, L.; Li, D. In *Prediction of dissolved oxygen content in aquaculture of Hyriopsis cumingii using Elman neural network*, International Conference on Computer and Computing Technologies in Agriculture, 2011; Springer: pp 508-518.
3. Heddam, S.; Kisi, O., Extreme learning machines: a new approach for modeling dissolved oxygen (DO) concentration with and without water quality variables as predictors. *Environmental Science and Pollution Research* **2017**, 24, (20), 16702-16724.
4. Li, C.; Li, Z.; Wu, J.; Zhu, L.; Yue, J., A hybrid model for dissolved oxygen prediction in aquaculture based on multi-scale features. *Information processing in agriculture* **2018**, 5, (1), 11-20.
5. Ay, M.; Kisi, O., Modeling of dissolved oxygen concentration using different neural network techniques in Foundation Creek, El Paso County, Colorado. *Journal of Environmental Engineering* **2012**, 138, (6), 654-662.
6. Elkiran, G.; Nourani, V.; Abba, S.; Abdullahi, J., Artificial intelligence-based approaches for multi-station modelling of dissolve oxygen in river. *Global Journal of Environmental Science and Management* **2018**, 4, (4), 439-450.
7. Liu, Z.; Shao, J.; Xu, W.; Chen, H.; Zhang, Y., An extreme learning machine approach for slope stability evaluation and prediction. *Natural hazards* **2014**, 73, (2), 787-804.
8. Liu, J.; Wu, C.; Wu, G.; Wang, X., A novel differential search algorithm and applications for structure design. *Applied Mathematics and Computation* **2015**, 268, 246-269.
9. Chen, Y.; He, L.; Li, J.; Zhang, S., Multi-criteria design of shale-gas-water supply chains and production systems towards optimal life cycle economics and greenhouse gas emissions under uncertainty. *Computers & Chemical Engineering* **2018**, 109, 216-235.
10. Zhu, J.; Shi, Q.; Wu, P.; Sheng, Z.; Wang, X., Complexity analysis of prefabrication contractors' dynamic price competition in mega projects with different competition strategies. *Complexity* **2018**, 2018.
11. Hu, X.; Chong, H.-Y.; Wang, X., Sustainability perceptions of off-site manufacturing stakeholders in Australia. *Journal of Cleaner Production* **2019**, 227, 346-354.
12. Zhang, K.; Wang, Q.; Chao, L.; Ye, J.; Li, Z.; Yu, Z.; Yang, T.; Ju, Q., Ground observation-based analysis of soil moisture spatiotemporal variability across a humid to semi-humid transitional zone in China. *Journal of Hydrology* **2019**, 574, 903-914.
13. Wang, M.; Chen, H., Chaotic multi-swarm whale optimizer boosted support vector machine for medical diagnosis. *Applied Soft Computing Journal* **2020**, 88.
14. Li, C.; Hou, L.; Sharma, B. Y.; Li, H.; Chen, C.; Li, Y.; Zhao, X.; Huang, H.; Cai, Z.; Chen, H., Developing a new intelligent system for the diagnosis of tuberculous pleural effusion. *Computer methods and programs in biomedicine* **2018**, 153, 211-225.
15. Feng, S.; Lu, H.; Tian, P.; Xue, Y.; Lu, J.; Tang, M.; Feng, W., Analysis of microplastics in a remote region of the Tibetan Plateau: Implications for natural environmental response to human activities. *Science of The Total Environment* **2020**, 739, 140087.

16. Han, X.; Zhang, D.; Yan, J.; Zhao, S.; Liu, J., Process development of flue gas desulphurization wastewater treatment in coal-fired power plants towards zero liquid discharge: Energetic, economic and environmental analyses. *Journal of Cleaner Production* **2020**, 261, 121144.
17. He, L.; Chen, Y.; Zhao, H.; Tian, P.; Xue, Y.; Chen, L., Game-based analysis of energy-water nexus for identifying environmental impacts during Shale gas operations under stochastic input. *Science of The Total Environment* **2018**, 627, 1585-1601.
18. He, L.; Shen, J.; Zhang, Y., Ecological vulnerability assessment for ecological conservation and environmental management. *Journal of Environmental Management* **2018**, 206, 1115-1125.
19. Liu, J.; Liu, Y.; Wang, X., An environmental assessment model of construction and demolition waste based on system dynamics: a case study in Guangzhou. *Environmental Science and Pollution Research* **2020**, 27, (30), 37237-37259.
20. Liu, L.; Li, J.; Yue, F.; Yan, X.; Wang, F.; Bloszies, S.; Wang, Y., Effects of arbuscular mycorrhizal inoculation and biochar amendment on maize growth, cadmium uptake and soil cadmium speciation in Cd-contaminated soil. *Chemosphere* **2018**, 194, 495-503.
21. Yang, Y.; Liu, J.; Yao, J.; Kou, J.; Li, Z.; Wu, T.; Zhang, K.; Zhang, L.; Sun, H., Adsorption behaviors of shale oil in kerogen slit by molecular simulation. *Chemical Engineering Journal* **2020**, 387, 124054.
22. Keshtegar, B.; Heddarn, S.; Sebbar, A.; Zhu, S.-P.; Trung, N.-T., SVR-RSM: a hybrid heuristic method for modeling monthly pan evaporation. *Environmental Science and Pollution Research* **2019**, 26, (35), 35807-35826.
23. Deng, Y.; Zhang, T.; Clark, J.; Aminabhavi, T.; Kruse, A.; Tsang, D. C.; Sharma, B. K.; Zhang, F.; Ren, H., Mechanisms and modelling of phosphorus solid-liquid transformation during the hydrothermal processing of swine manure. *Green Chemistry* **2020**, 22, (17), 5628-5638.
24. Zhang, B.; Xu, D.; Liu, Y.; Li, F.; Cai, J.; Du, L., Multi-scale evapotranspiration of summer maize and the controlling meteorological factors in north China. *Agricultural and Forest Meteorology* **2016**, 216, 1-12.
25. Chao, L.; Zhang, K.; Li, Z.; Zhu, Y.; Wang, J.; Yu, Z., Geographically weighted regression based methods for merging satellite and gauge precipitation. *Journal of Hydrology* **2018**, 558, 275-289.
26. Wang, Y.; Yuan, Y.; Wang, Q.; Liu, C.; Zhi, Q.; Cao, J., Changes in air quality related to the control of coronavirus in China: Implications for traffic and industrial emissions. *Science of The Total Environment* **2020**, 731, 139133.
27. Chen, Y.; He, L.; Guan, Y.; Lu, H.; Li, J., Life cycle assessment of greenhouse gas emissions and water-energy optimization for shale gas supply chain planning based on multi-level approach: Case study in Barnett, Marcellus, Fayetteville, and Haynesville shales. *Energy Conversion and Management* **2017**, 134, 382-398.
28. He, L.; Chen, Y.; Li, J., A three-level framework for balancing the tradeoffs among the energy, water, and air-emission implications within the life-cycle shale gas supply chains. *Resources, Conservation and Recycling* **2018**, 133, 206-228.
29. Lu, H.; Tian, P.; He, L., Evaluating the global potential of aquifer thermal energy storage and determining the potential worldwide hotspots driven by socio-economic, geo-hydrologic and climatic conditions. *Renewable and Sustainable Energy Reviews* **2019**, 112, 788-796.
30. Wang, Y.; Yao, M.; Ma, R.; Yuan, Q.; Yang, D.; Cui, B.; Ma, C.; Liu, M.; Hu, D., Design strategy of barium titanate/polyvinylidene fluoride-based nanocomposite films for high energy storage. *Journal of Materials Chemistry A* **2020**, 8, (3), 884-917.
31. Zhu, L.; Kong, L.; Zhang, C., Numerical Study on Hysteretic Behaviour of Horizontal-Connection and Energy-Dissipation Structures Developed for Prefabricated Shear Walls. *Applied Sciences* **2020**, 10, (4), 1240.
32. Zhao, X.; Ye, Y.; Ma, J.; Shi, P.; Chen, H., Construction of electric vehicle driving cycle for studying electric vehicle energy consumption and equivalent emissions. *Environmental Science and Pollution Research* **2020**, 1-15.
33. Deng, Y.; Zhang, T.; Sharma, B. K.; Nie, H., Optimization and mechanism studies on cell disruption and phosphorus recovery from microalgae with magnesium modified hydrochar in assisted hydrothermal system. *Science of The Total Environment* **2019**, 646, 1140-1154.

34. Zhang, T.; Wu, X.; Fan, X.; Tsang, D. C. W.; Li, G.; Shen, Y., Corn waste valorization to generate activated hydrochar to recover ammonium nitrogen from compost leachate by hydrothermal assisted pretreatment. *Journal of Environmental Management* **2019**, 236, 108-117.
35. Chen, Y.; Li, J.; Lu, H.; Yan, P., Coupling system dynamics analysis and risk aversion programming for optimizing the mixed noise-driven shale gas-water supply chains. *Journal of Cleaner Production* **2021**, 278, 123209.
36. Cheng, X.; He, L.; Lu, H.; Chen, Y.; Ren, L., Optimal water resources management and system benefit for the Marcellus shale-gas reservoir in Pennsylvania and West Virginia. *Journal of Hydrology* **2016**, 540, 412-422.
37. Li, L.-L.; Liu, Y.-W.; Tseng, M.-L.; Lin, G.-Q.; Ali, M. H., Reducing environmental pollution and fuel consumption using optimization algorithm to develop combined cooling heating and power system operation strategies. *Journal of Cleaner Production* **2020**, 247, 119082.
38. Li, X.; Zhang, R.; Zhang, X.; Zhu, P.; Yao, T., Silver-Catalyzed Decarboxylative Allylation of Difluoroarylacetic Acids with Allyl Sulfones in Water. *Chemistry – An Asian Journal* **2020**, 15, (7), 1175-1179.
39. Yang, M.; Sowmya, A., An Underwater Color Image Quality Evaluation Metric. *IEEE Transactions on Image Processing* **2015**, 24, (12), 6062-6071.
40. Cao, B.; Fan, S.; Zhao, J.; Yang, P.; Muhammad, K.; Tanveer, M., Quantum-enhanced multiobjective large-scale optimization via parallelism. *Swarm and Evolutionary Computation* **2020**, 57, 100697.
41. Qian, J.; Feng, S.; Li, Y.; Tao, T.; Han, J.; Chen, Q.; Zuo, C., Single-shot absolute 3D shape measurement with deep-learning-based color fringe projection profilometry. *Optics Letters* **2020**, 45, (7), 1842-1845.
42. Lyu, Z.; Chai, J.; Xu, Z.; Qin, Y.; Cao, J., A Comprehensive Review on Reasons for Tailings Dam Failures Based on Case History. *Advances in Civil Engineering* **2019**, 2019, 4159306.
43. Feng, W.; Lu, H.; Yao, T.; Yu, Q., Drought characteristics and its elevation dependence in the Qinghai-Tibet plateau during the last half-century. *Scientific Reports* **2020**, 10, (1), 14323.
44. Su, Z.; Liu, E.; Xu, Y.; Xie, P.; Shang, C.; Zhu, Q., Flow field and noise characteristics of manifold in natural gas transportation station. *Oil & Gas Science and Technology—Revue d'IFP Energies nouvelles* **2019**, 74, 70.
45. Shi, K.; Wang, J.; Tang, Y.; Zhong, S., Reliable asynchronous sampled-data filtering of T-S fuzzy uncertain delayed neural networks with stochastic switched topologies. *Fuzzy Sets and Systems* **2020**, 381, 1-25.
46. Shi, K.; Wang, J.; Zhong, S.; Tang, Y.; Cheng, J., Non-fragile memory filtering of T-S fuzzy delayed neural networks based on switched fuzzy sampled-data control. *Fuzzy Sets and Systems* **2020**, 394, 40-64.
47. Wang, S.-J.; Chen, H.-L.; Yan, W.-J.; Chen, Y.-H.; Fu, X., Face recognition and micro-expression recognition based on discriminant tensor subspace analysis plus extreme learning machine. *Neural processing letters* **2014**, 39, (1), 25-43.
48. Mi, C.; Cao, L.; Zhang, Z.; Feng, Y.; Yao, L.; Wu, Y., A port container code recognition algorithm under natural conditions. *Journal of Coastal Research* **2020**, 103, (SI), 822-829.
49. Salari, N.; Shohaimi, S.; Najafi, F.; Nallappan, M.; Karishnarajah, I., Application of pattern recognition tools for classifying acute coronary syndrome: an integrated medical modeling. *Theoretical Biology and Medical Modelling* **2013**, 10, (1), 57.
50. Yue, H.; Wang, H.; Chen, H.; Cai, K.; Jin, Y., Automatic detection of feather defects using Lie group and fuzzy Fisher criterion for shuttlecock production. *Mechanical Systems and Signal Processing* **2020**, 141, 106690.
51. Xu, M.; Li, C.; Zhang, S.; Callet, P. L., State-of-the-Art in 360° Video/Image Processing: Perception, Assessment and Compression. *IEEE Journal of Selected Topics in Signal Processing* **2020**, 14, (1), 5-26.
52. Zenggang, X.; Zhiwen, T.; Xiaowen, C.; Xue-min, Z.; Kaibin, Z.; Conghuan, Y., Research on Image Retrieval Algorithm Based on Combination of Color and Shape Features. *Journal of Signal Processing Systems* **2019**, 1-8.
53. Zhu, Q., Research on Road Traffic Situation Awareness System Based on Image Big Data. *IEEE Intelligent Systems* **2020**, 35, (1), 18-26.
54. Xu, S.; Wang, J.; Shou, W.; Ngo, T.; Sadick, A.-M.; Wang, X., Computer Vision Techniques in Construction: A Critical Review. *Archives of Computational Methods in Engineering* **2020**.

55. Yan, J.; Pu, W.; Zhou, S.; Liu, H.; Bao, Z., Collaborative detection and power allocation framework for target tracking in multiple radar system. *Information Fusion* **2020**, 55, 173-183.
56. Chao, M.; Kai, C.; Zhiwei, Z., Research on tobacco foreign body detection device based on machine vision. *Transactions of the Institute of Measurement and Control* **2020**, 42, (15), 2857-2871.
57. Chen, H.-L.; Wang, G.; Ma, C.; Cai, Z.-N.; Liu, W.-B.; Wang, S.-J. J. N., An efficient hybrid kernel extreme learning machine approach for early diagnosis of Parkinson' s disease. *Neurocomputing* **2016**, 184, 131-144.
58. Zhang, C.; Wang, H., Swing vibration control of suspended structures using the Active Rotary Inertia Driver system: Theoretical modeling and experimental verification. *Structural Control and Health Monitoring* **2020**, 27, (6), e2543.
59. Zhang, C.-W.; Ou, J.-P.; Zhang, J.-Q., Parameter optimization and analysis of a vehicle suspension system controlled by magnetorheological fluid dampers. *Structural Control and Health Monitoring* **2006**, 13, (5), 885-896.
60. Yang, W.; Pudasainee, D.; Gupta, R.; Li, W.; Wang, B.; Sun, L., An overview of inorganic particulate matter emission from coal/biomass/MSW combustion: Sampling and measurement, formation, distribution, inorganic composition and influencing factors. *Fuel Processing Technology* **2020**, 106657.
61. Abedini, M.; Mutalib, A. A.; Zhang, C.; Mehrmashhadi, J.; Raman, S. N.; Alipour, R.; Momeni, T.; Mussa, M. H., Large deflection behavior effect in reinforced concrete columns exposed to extreme dynamic loads. *Frontiers of Structural and Civil Engineering* **2020**, 14, (2), 532-553.
62. Mou, B.; Li, X.; Bai, Y.; Wang, L., Shear behavior of panel zones in steel beam-to-column connections with unequal depth of outer annular stiffener. *Journal of Structural Engineering* **2019**, 145, (2), 04018247.
63. Mou, B.; Zhao, F.; Qiao, Q.; Wang, L.; Li, H.; He, B.; Hao, Z., Flexural behavior of beam to column joints with or without an overlying concrete slab. *Engineering Structures* **2019**, 199, 109616.
64. Abedini, M.; Zhang, C., Performance Assessment of Concrete and Steel Material Models in LS-DYNA for Enhanced Numerical Simulation, A State of the Art Review. *Archives of Computational Methods in Engineering* **2020**.
65. Gholipour, G.; Zhang, C.; Mousavi, A. A., Numerical analysis of axially loaded RC columns subjected to the combination of impact and blast loads. *Engineering Structures* **2020**, 219, 110924.
66. Zhang, C.; Abedini, M.; Mehrmashhadi, J., Development of pressure-impulse models and residual capacity assessment of RC columns using high fidelity Arbitrary Lagrangian-Eulerian simulation. *Engineering Structures* **2020**, 224, 111219.
67. Zhang, Y.; Liu, R.; Wang, X.; Chen, H.; Li, C., Boosted binary Harris hawks optimizer and feature selection. *Engineering with Computers* **2020**.
68. Wang, S.; Zhang, K.; van Beek, L. P. H.; Tian, X.; Bogaard, T. A., Physically-based landslide prediction over a large region: Scaling low-resolution hydrological model results for high-resolution slope stability assessment. *Environmental Modelling & Software* **2020**, 124, 104607.
69. Pourya, K.; Abdolreza, O.; Brent, V.; Arash, H.; Hamid, R. In *Feasibility Study of Collapse Remediation of Illinois Loess Using Electrokinetics Technique by Nanosilica and Salt*, Geo-Congress 2020, 2020; pp 667-675.
70. Baziar, M. H.; Rostami, H., Earthquake Demand Energy Attenuation Model for Liquefaction Potential Assessment. *Earthquake Spectra* **2017**, 33, (2), 757-780.
71. Ebrahimi, M.; Moradi, A.; Bejvani, M.; Davatgari Tafreshi, M. In *Application of STA/LTA Based on Cross-Correlation to Passive Seismic Data*, Sixth EAGE Workshop on Passive Seismic, Muscat, Oman, January 31-February 3, 2016, 2016; Muscat, Oman, pp 1-5.
72. Ebrahimi, M.; Taleshi, A. A.; Abbasinia, M.; Arab-Amiri, A., Two and three-dimonsional ERT modelling for a buried tunnel. *Journal of Emerging Trends in Engineering and Applied Sciences* **2016**, 7, (3), 118-127.
73. Qian, J.; Feng, S.; Tao, T.; Hu, Y.; Li, Y.; Chen, Q.; Zuo, C., Deep-learning-enabled geometric constraints and phase unwrapping for single-shot absolute 3D shape measurement. *APL Photonics* **2020**, 5, (4), 046105.
74. Xiong, Q.; Zhang, X.; Wang, W.-F.; Gu, Y., A Parallel Algorithm Framework for Feature Extraction of EEG Signals on MPI. *Computational and Mathematical Methods in Medicine* **2020**, 2020, 9812019.
75. Xiong, Z.; Xiao, N.; Xu, F.; Zhang, X.; Xu, Q.; Zhang, K.; Ye, C., An Equivalent Exchange Based Data Forwarding Incentive Scheme for Socially Aware Networks. *Journal of Signal Processing Systems* **2020**.

76. Zhu, G.; Wang, S.; Sun, L.; Ge, W.; Zhang, X., Output Feedback Adaptive Dynamic Surface Sliding-Mode Control for Quadrotor UAVs with Tracking Error Constraints. *Complexity* **2020**, 2020, 8537198.
77. Zhang, J.; Liu, B., A review on the recent developments of sequence-based protein feature extraction methods. *Current Bioinformatics* **2019**, 14, (3), 190-199.
78. Zhao, X.; Li, D.; Yang, B.; Chen, H.; Yang, X.; Yu, C.; Liu, S., A two-stage feature selection method with its application. *Computers & Electrical Engineering* **2015**, 47, 114-125.
79. Chen, H.; Chen, A.; Xu, L.; Xie, H.; Qiao, H.; Lin, Q.; Cai, K., A deep learning CNN architecture applied in smart near-infrared analysis of water pollution for agricultural irrigation resources. *Agricultural Water Management* **2020**, 240, 106303.
80. Liu, E.; Lv, L.; Yi, Y.; Xie, P., Research on the Steady Operation Optimization Model of Natural Gas Pipeline Considering the Combined Operation of Air Coolers and Compressors. *IEEE Access* **2019**, 7, 83251-83265.
81. Lv, Z.; Qiao, L., Deep belief network and linear perceptron based cognitive computing for collaborative robots. *Applied Soft Computing* **2020**, 92, 106300.
82. Qiu, T.; Shi, X.; Wang, J.; Li, Y.; Qu, S.; Cheng, Q.; Cui, T.; Sui, S., Deep Learning: A Rapid and Efficient Route to Automatic Metasurface Design. *Advanced Science* **2019**, 6, (12), 1900128.
83. Xu, M.; Li, T.; Wang, Z.; Deng, X.; Yang, R.; Guan, Z., Reducing Complexity of HEVC: A Deep Learning Approach. *IEEE Transactions on Image Processing* **2018**, 27, (10), 5044-5059.
84. Liu, S.; Chan, F. T. S.; Ran, W., Decision making for the selection of cloud vendor: An improved approach under group decision-making with integrated weights and objective/subjective attributes. *Expert Systems with Applications* **2016**, 55, 37-47.
85. Tian, P.; Lu, H.; Feng, W.; Guan, Y.; Xue, Y., Large decrease in streamflow and sediment load of Qinghai-Tibetan Plateau driven by future climate change: A case study in Lhasa River Basin. *CATENA* **2020**, 187, 104340.
86. Cao, B.; Dong, W.; Lv, Z.; Gu, Y.; Singh, S.; Kumar, P., Hybrid Microgrid Many-Objective Sizing Optimization With Fuzzy Decision. *IEEE Transactions on Fuzzy Systems* **2020**, 28, (11), 2702-2710.
87. Cao, B.; Zhao, J.; Gu, Y.; Ling, Y.; Ma, X., Applying graph-based differential grouping for multiobjective large-scale optimization. *Swarm and Evolutionary Computation* **2020**, 53, 100626.
88. Qu, S.; Han, Y.; Wu, Z.; Raza, H., Consensus Modeling with Asymmetric Cost Based on Data-Driven Robust Optimization. *Group Decision and Negotiation* **2020**.
89. Wu, C.; Wu, P.; Wang, J.; Jiang, R.; Chen, M.; Wang, X., Critical review of data-driven decision-making in bridge operation and maintenance. *Structure and Infrastructure Engineering* **2020**, 1-24.
90. Cao, B.; Zhao, J.; Lv, Z.; Gu, Y.; Yang, P.; Halgamuge, S. K., Multiobjective Evolution of Fuzzy Rough Neural Network via Distributed Parallelism for Stock Prediction. *IEEE Transactions on Fuzzy Systems* **2020**, 28, (5), 939-952.
91. Cao, B.; Zhao, J.; Gu, Y.; Fan, S.; Yang, P., Security-Aware Industrial Wireless Sensor Network Deployment Optimization. *IEEE Transactions on Industrial Informatics* **2020**, 16, (8), 5309-5316.
92. Chen, H.; Qiao, H.; Xu, L.; Feng, Q.; Cai, K., A Fuzzy Optimization Strategy for the Implementation of RBF LSSVR Model in Vis-NIR Analysis of Pomelo Maturity. *IEEE Transactions on Industrial Informatics* **2019**, 15, (11), 5971-5979.
93. Fu, X.; Pace, P.; Aloï, G.; Yang, L.; Fortino, G., Topology Optimization Against Cascading Failures on Wireless Sensor Networks Using a Memetic Algorithm. *Computer Networks* **2020**, 177, (4 August 2020), 107327.
94. Adeli, H., Neural networks in civil engineering: 1989-2000. *Computer-Aided Civil and Infrastructure Engineering* **2001**, 16, (2), 126-142.
95. Hornik, K.; Stinchcombe, M.; White, H., Multilayer feedforward networks are universal approximators. *Neural networks* **1989**, 2, (5), 359-366.
96. Li, Z.-G.; Cheng, H.; Gu, T.-Y., Research on dynamic relationship between natural gas consumption and economic growth in China. *Structural Change and Economic Dynamics* **2019**, 49, 334-339.
97. Yang, J.; Li, S.; Wang, Z.; Dong, H.; Wang, J.; Tang, S., Using Deep Learning to Detect Defects in Manufacturing: A Comprehensive Survey and Current Challenges. *Materials* **2020**, 13, (24).
98. Yu, H.; Li, W.; Chen, C.; Liang, J.; Gui, W.; Wang, M.; Chen, H. J. E. w. C., Dynamic Gaussian bare-bones fruit fly optimizers with abandonment mechanism: method and analysis. *Engineering with Computers* **2020**, 1-29.

99. Chen, H.-L.; Wang, G.; Ma, C.; Cai, Z.-N.; Liu, W.-B.; Wang, S.-J., An efficient hybrid kernel extreme learning machine approach for early diagnosis of Parkinson' s disease. *Neurocomputing* **2016**, 184, 131-144.
100. Hu, L.; Hong, G.; Ma, J.; Wang, X.; Chen, H., An efficient machine learning approach for diagnosis of paraquat-poisoned patients. *Computers in Biology and Medicine* **2015**, 59, 116-124.
101. Xia, J.; Chen, H.; Li, Q.; Zhou, M.; Chen, L.; Cai, Z.; Fang, Y.; Zhou, H., Ultrasound-based differentiation of malignant and benign thyroid Nodules: An extreme learning machine approach. *Computer methods and programs in biomedicine* **2017**, 147, 37-49.
102. Zhao, X.; Zhang, X.; Cai, Z.; Tian, X.; Wang, X.; Huang, Y.; Chen, H.; Hu, L., Chaos enhanced grey wolf optimization wrapped ELM for diagnosis of paraquat-poisoned patients. *Computational Biology and Chemistry* **2019**, 78, 481-490.
103. Cao, B.; Zhao, J.; Yang, P.; Gu, Y.; Muhammad, K.; Rodrigues, J. J. P. C.; Albuquerque, V. H. C. d., Multiobjective 3-D Topology Optimization of Next-Generation Wireless Data Center Network. *IEEE Transactions on Industrial Informatics* **2020**, 16, (5), 3597-3605.
104. Cao, B.; Wang, X.; Zhang, W.; Song, H.; Lv, Z., A Many-Objective Optimization Model of Industrial Internet of Things Based on Private Blockchain. *IEEE Network* **2020**, 34, (5), 78-83.
105. Shen, L.; Chen, H.; Yu, Z.; Kang, W.; Zhang, B.; Li, H.; Yang, B.; Liu, D., Evolving support vector machines using fruit fly optimization for medical data classification. *Knowledge-Based Systems* **2016**, 96, 61-75.
106. Zhao, X.; Li, D.; Yang, B.; Ma, C.; Zhu, Y.; Chen, H., Feature selection based on improved ant colony optimization for online detection of foreign fiber in cotton. *Applied Soft Computing* **2014**, 24, 585-596.
107. Wang, M.; Chen, H.; Yang, B.; Zhao, X.; Hu, L.; Cai, Z.; Huang, H.; Tong, C., Toward an optimal kernel extreme learning machine using a chaotic moth-flame optimization strategy with applications in medical diagnoses. *Neurocomputing* **2017**, 267, 69-84.
108. Xu, X.; Chen, H.-L., Adaptive computational chemotaxis based on field in bacterial foraging optimization. *Soft Computing* **2014**, 18, (4), 797-807.
109. Xu, Y.; Chen, H.; Luo, J.; Zhang, Q.; Jiao, S.; Zhang, X., Enhanced Moth-flame optimizer with mutation strategy for global optimization. *Information Sciences* **2019**, 492, 181-203.
110. Zhang, X.; Jiang, R.; Wang, T.; Wang, J., Recursive Neural Network for Video Deblurring. *IEEE Transactions on Circuits and Systems for Video Technology* **2020**, 1-1.
111. Zhang, X.; Wang, T.; Wang, J.; Tang, G.; Zhao, L., Pyramid Channel-based Feature Attention Network for image dehazing. *Computer Vision and Image Understanding* **2020**, 197-198, 103003.
112. Li, W.; Fang, H.; Qin, G.; Tan, X.; Huang, Z.; Zeng, F.; Du, H.; Li, S., Concentration estimation of dissolved oxygen in Pearl River Basin using input variable selection and machine learning techniques. *Science of The Total Environment* **2020**, 139099.
113. Csábrági, A.; Molnár, S.; Tanos, P.; Kovács, J., Application of artificial neural networks to the forecasting of dissolved oxygen content in the Hungarian section of the river Danube. *Ecological Engineering* **2017**, 100, 63-72.
114. Csábrági, A.; Molnár, S.; Tanos, P.; Kovács, J.; Molnár, M.; Szabó, I.; Hatvani, I. G., Estimation of dissolved oxygen in riverine ecosystems: Comparison of differently optimized neural networks. *Ecological Engineering* **2019**, 138, 298-309.
115. Heddam, S., Simultaneous modelling and forecasting of hourly dissolved oxygen concentration (DO) using radial basis function neural network (RBFNN) based approach: a case study from the Klamath River, Oregon, USA. *Modeling Earth Systems and Environment* **2016**, 2, (3), 135.
116. Heddam, S., Fuzzy neural network (EFuNN) for modelling dissolved oxygen concentration (DO). In *Intelligence Systems in Environmental Management: Theory and Applications*, Springer: 2017; pp 231-253.
117. Khan, U. T.; Valeo, C., Dissolved oxygen prediction using a possibility theory based fuzzy neural network. *Hydrology and Earth System Sciences* **2016**, 20, (6), 2267.
118. Ahmed, A. M.; Shah, S. M. A., Application of adaptive neuro-fuzzy inference system (ANFIS) to estimate the biochemical oxygen demand (BOD) of Surma River. *Journal of King Saud University-Engineering Sciences* **2017**, 29, (3), 237-243.
119. Heddam, S., Modeling hourly dissolved oxygen concentration (DO) using two different adaptive neuro-fuzzy inference systems (ANFIS): a comparative study. *Environmental Monitoring and Assessment* **2014**, 186, (1), 597-619.

120. Ranković, V.; Radulović, J.; Radojević, I.; Ostojić, A.; Čomić, L., Prediction of dissolved oxygen in reservoirs using adaptive network-based fuzzy inference system. *Journal of Hydroinformatics* **2012**, 14, (1), 167-179.
121. Heddam, S.; Kisi, O., Modelling daily dissolved oxygen concentration using least square support vector machine, multivariate adaptive regression splines and M5 model tree. *Journal of Hydrology* **2018**, 559, 499-509.
122. Kisi, O.; Akbari, N.; Sanatipour, M.; Hashemi, A.; Teimourzadeh, K.; Shiri, J., Modeling of Dissolved Oxygen in River Water Using Artificial Intelligence Techniques. *Journal of Environmental Informatics* **2013**, 22, (2).
123. Li, X.; Sha, J.; Wang, Z.-l., A comparative study of multiple linear regression, artificial neural network and support vector machine for the prediction of dissolved oxygen. *Hydrology Research* **2017**, 48, (5), 1214-1225.
124. Antanasijević, D.; Pocajt, V.; Perić-Grujić, A.; Ristić, M., Modelling of dissolved oxygen in the Danube River using artificial neural networks and Monte Carlo Simulation uncertainty analysis. *Journal of Hydrology* **2014**, 519, 1895-1907.
125. Ouma, Y. O.; Okuku, C. O.; Njau, E. N., Use of Artificial Neural Networks and Multiple Linear Regression Model for the Prediction of Dissolved Oxygen in Rivers: Case Study of Hydrographic Basin of River Nyando, Kenya. *Complexity* **2020**, 2020.
126. Lu, H.; Ma, X., Hybrid decision tree-based machine learning models for short-term water quality prediction. *Chemosphere* **2020**, 249, 126169.
127. Ahmed, M. H., Prediction of the Concentration of Dissolved Oxygen in Running Water by Employing A Random Forest Machine Learning Technique. **2020**.
128. Ay, M.; Kişi, Ö., Estimation of dissolved oxygen by using neural networks and neuro fuzzy computing techniques. *KSCE Journal of Civil Engineering* **2017**, 21, (5), 1631-1639.
129. Rajaei, T.; Khani, S.; Ravansalar, M., Artificial intelligence-based single and hybrid models for prediction of water quality in rivers: A review. *Chemometrics and Intelligent Laboratory Systems* **2020**, 103978.
130. Faruk, D. Ö., A hybrid neural network and ARIMA model for water quality time series prediction. *Engineering applications of artificial intelligence* **2010**, 23, (4), 586-594.
131. Bui, D. T.; Khosravi, K.; Tiefenbacher, J.; Nguyen, H.; Kazakis, N., Improving prediction of water quality indices using novel hybrid machine-learning algorithms. *Science of The Total Environment* **2020**, 137612.
132. Ravansalar, M.; Rajaei, T.; Ergil, M., Prediction of dissolved oxygen in River Calder by noise elimination time series using wavelet transform. *Journal of Experimental & Theoretical Artificial Intelligence* **2016**, 28, (4), 689-706.
133. Antanasijević, D.; Pocajt, V.; Perić-Grujić, A.; Ristić, M., Multilevel split of high-dimensional water quality data using artificial neural networks for the prediction of dissolved oxygen in the Danube River. *Neural Computing and Applications* **2019**, 1-10.
134. Nacar, S.; Bayram, A.; Baki, O. T.; Kankal, M.; Aras, E., Spatial Forecasting of Dissolved Oxygen Concentration in the Eastern Black Sea Basin, Turkey. *Water* **2020**, 12, (4), 1041.
135. Mahmoudi, N.; Orouji, H.; Fallah-Mehdipour, E., Integration of shuffled frog leaping algorithm and support vector regression for prediction of water quality parameters. *Water resources management* **2016**, 30, (7), 2195-2211.
136. Zhu, C.; Liu, X.; Ding, W. In *Prediction model of dissolved oxygen based on FOA-LSSVR*, 2017 36th Chinese Control Conference (CCC), 2017; IEEE: pp 9819-9823.
137. Raheli, B.; Aalami, M. T.; El-Shafie, A.; Ghorbani, M. A.; Deo, R. C., Uncertainty assessment of the multilayer perceptron (MLP) neural network model with implementation of the novel hybrid MLP-FFA method for prediction of biochemical oxygen demand and dissolved oxygen: a case study of Langat River. *Environmental Earth Sciences* **2017**, 76, (14), 503.
138. Deng, C.; Wei, X.; Guo, L. In *Application of neural network based on PSO algorithm in prediction model for dissolved oxygen in fishpond*, 2006 6th World Congress on Intelligent Control and Automation, 2006; IEEE: pp 9401-9405.
139. Barrow, J. D.; Davies, P. C.; Harper Jr, C. L., *Science and ultimate reality: Quantum theory, cosmology, and complexity*. Cambridge University Press: 2004.

140. Mirjalili, S.; Mirjalili, S. M.; Hatamlou, A., Multi-verse optimizer: a nature-inspired algorithm for global optimization. *Neural Computing and Applications* **2016**, 27, (2), 495-513.
141. Abasi, A. K.; Khader, A. T.; Al-Betar, M. A.; Naim, S.; Makhadmeh, S. N.; Alyasseri, Z. A. A., Link-based multi-verse optimizer for text documents clustering. *Applied Soft Computing* **2020**, 87, 106002.
142. Faris, H.; Hassonah, M. A.; Ala'M, A.-Z.; Mirjalili, S.; Aljarah, I., A multi-verse optimizer approach for feature selection and optimizing SVM parameters based on a robust system architecture. *Neural Computing and Applications* **2018**, 30, (8), 2355-2369.
143. Hatamlou, A., Black hole: A new heuristic optimization approach for data clustering. *Information sciences* **2013**, 222, 175-184.
144. Qasim, O. S.; Al-Thanoon, N. A.; Algarni, Z. Y., Feature selection based on chaotic binary black hole algorithm for data classification. *Chemometrics and Intelligent Laboratory Systems* **2020**, 104104.
145. Duan, Q.; Gupta, V. K.; Sorooshian, S., Shuffled complex evolution approach for effective and efficient global minimization. *Journal of optimization theory and applications* **1993**, 76, (3), 501-521.
146. Majeed, K.; Qyyum, M. A.; Nawaz, A.; Ahmad, A.; Naqvi, M.; He, T.; Lee, M., Shuffled Complex Evolution-Based Performance Enhancement and Analysis of Cascade Liquefaction Process for Large-Scale LNG Production. *Energies* **2020**, 13, (10), 2511.